

Bistable Goos-Hänchen shift owing to leaky-mode excitation in a slab waveguide with Kerr nonlinear medium

Yuan-Ping Cai(蔡园平), Li Jiang(姜丽), and Ren-Gang Wan(万仁刚)
Citation: Chin. Phys. B, 2026, 35 (**4**): 044203. DOI: 10.1088/1674-1056/ae00b3
http://cpb.iphy.ac.cn; http://iopscience.iop.org/cpb

What follows is a list of articles you may be interested in

Controllable optical bistability in a Fabry-Pérot cavity with a nonlinear three-dimensional Dirac semimetal

Hong-Xia Yuan(袁红霞), Jia-Xue Li(李佳雪), Qi-Jun Ma(马奇军), Hai-Shan Tian(田海山),Yun-Yang Ye(叶云洋), Wen-Xin Luo(罗文昕), Xing-Hua Wu(吴杏华), and Le-Yong Jiang(蒋乐勇)
Chin. Phys. B, 2024, 33 (**3**): 034213. DOI: 10.1088/1674-1056/acfdfe

Low-threshold bistable reflection assisted by oscillating wave interaction with Kerr nonlinear medium

Yingcong Zhang(张颖聪), Wenjuan Cai(蔡文娟), Xianping Wang(王贤平), Wen Yuan(袁文), Cheng Yin(殷澄), Jun Li(李俊), Haimei Luo(罗海梅), and Minghuang Sang(桑明煌)
Chin. Phys. B, 2021, 30 (**8**): 084203. DOI: 10.1088/1674-1056/abe118

Electro-optomechanical switch via tunable bistability and four-wave mixing

Kamran Ullah
Chin. Phys. B, 2019, 28 (**11**): 114209. DOI: 10.1088/1674-1056/ab4580

Controllable optical bistability in a three-mode optomechanical system with a membrane resonator

Jiakai Yan(闫甲楷), Xiaofei Zhu(朱小霏), Bin Chen(陈彬)
Chin. Phys. B, 2018, 27 (**7**): 074214. DOI: 10.1088/1674-1056/27/7/074214

High contrast all-optical diode based on direction-dependent optical bistability within asymmetric ring cavity

Xiu-Wen Xia(夏秀文), Xin-Qin Zhang(张新琴), Jing-Ping Xu(许静平), Ya-Ping Yang(羊亚平)
Chin. Phys. B, 2016, 25 (**8**): 084211. DOI: 10.1088/1674-1056/25/8/084211

Bistable Goos–Hänchen shift owing to leaky-mode excitation in a slab waveguide with Kerr nonlinear medium

Yuan-Ping Cai(蔡园平)[1], Li Jiang(姜丽)[2,†], and Ren-Gang Wan(万仁刚)[1,‡]

[1] *School of Physics and Information Technology, Shaanxi Normal University, Xi'an* 710062, *China*
[2] *Changchun University of Science and Technology, Changchun* 130000, *China*

(Received 1 August 2025; revised manuscript received 25 August 2025; accepted manuscript online 29 August 2025)

We investigate the nonlinear Goos–Hänchen shift of a light beam reflected from a prism-coupled leaky waveguide containing a Kerr medium. As the incident power varies, the system can switch between two states, total internal reflection and frustrated total reflection, owing to the inherent positive feedback arising from the intensity-dependent guiding mode resonance. The reflectance exhibits optical bistability; meanwhile, the lateral shift of the reflected beam also shows hysteresis behavior. It is found that the transition between the two stable states is related to the excitation of a leaky mode in the waveguide, which results from the modulation of the electric field in the nonlinear substrate. We also analyze the effects of system parameters on the bistable Goos–Hänchen shift. The thresholds as well as the width of the hysteresis curve are sensitive to the thicknesses of the gap layer and the guiding layer, which determine the resonance angle. The bistable lateral displacement in the slab waveguide may have potential applications in optical switching, beam steering, etc.

Keywords: Goos–Hänchen shift, optical bistability, waveguide, nonlinear optics

PACS: 42.65.–k, 78.67.Pt, 78.20.Ci

DOI: 10.1088/1674-1056/ae00b3 **CSTR:** 32038.14.CPB.ae00b3

1. Introduction

In 1947, Goos and Hänchen[1] experimentally observed a lateral displacement of a light beam deviating from the position predicted by geometrical optics, and Artmann[2] subsequently provided a theoretical explanation of the Goos–Hänchen (GH) effect. When a light beam with finite width impinges on the boundary between two media, each plane-wave component with a slight difference in the transverse wave vector undergoes a different phase shift after reflection. The reflected beam, a superposition of all the components with different phases, is then laterally displaced in the plane of incidence. The GH shift in the total reflection scheme is relatively small. Therefore, the enhancement of lateral displacement has attracted much attention owing to its potential applications in optical sensing,[3–5] optical switching,[6,7] and beam steering.[8] Large and tunable GH shifts have been obtained in reflected and transmitted light beams incident on the interfaces of different materials and multilayered structures, such as negative materials,[9] dielectric slabs,[10] absorbing and gain media,[11,12] photonic crystals,[13] graphene,[14–16] surface plasmon resonance (SPR),[17–20] optical waveguides,[21–25] cavity-coupled coherent media,[26–28] and multilayer structures with quasi-bound states.[29,30]

Optical bistability, a typical nonlinear optical phenomenon, arises from the third-order nonlinearity of media and the feedback from an optical cavity. It was first investigated in two-level atomic systems in the early 1980s.[31] In recent years, the optical manipulation of bistability via multilevel coherent media, which provides more flexibility for controlling light by light, has attracted great interest.[32] On the other hand, many schemes of optical bistability produced by light reflected from multilayer structures containing nonlinear materials have been proposed without the requirement of an optical cavity. The bistable reflection is due to the excitation of surface-plasmon modes[33–36] and waveguide modes.[37,38] There also exists a hysteretic response between the GH shift and the incident intensity of the light beam. The bistable lateral displacement has been investigated in systems with surface plasmon resonance.[15,18,35,39,40] However, to the best of our knowledge, there has been little investigation of the bistable GH shift in a leaky slab waveguide. Moreover, the variation and distribution of the electric field in the case of optical bistability in planar waveguides have not been well studied.

In this paper, the bistable behavior of the GH shift is investigated in a prism-coupled leaky waveguide structure with a Kerr nonlinear substrate. In the case of guiding-mode resonance, a sharp dip occurs in the reflection spectrum, accompanied by a steep variation of phase shift and an enhancement of the evanescent electromagnetic wave in the substrate. When the guiding mode is out of resonance, the light beam undergoes total reflection with a small phase shift. Owing to the intensity-dependent waveguide-mode resonance induced by the nonlin-

[†]Corresponding author. E-mail: jiangli@cust.edu.cn
[‡]Corresponding author. E-mail: wrg@snnu.edu.cn

© 2026 Chinese Physical Society and IOP Publishing Ltd. All rights, including for text and data mining, AI training, and similar technologies, are reserved.

ear substrate, the system can be switched between two stable states: total internal reflection (TIR) and frustrated total reflection (FTR). As a result, the lateral displacement, which is related to the angular variation of the reflected phase, exhibits a hysteretic feature. The distribution of the electric field in the four-layer structure explains the formation of the bistable behavior. The effects of the thicknesses of the gap layer and the guiding layer, as well as the incident angle, on the bistable GH shift are also discussed in detail.

2. Model and equations

Figure 1 shows a prism-coupled planar waveguide structure. It consists of a ZF7 glass prism, an air gap layer with thickness d_1, a polymer guiding layer with thickness d_2, and a Kerr-type nonlinear substrate, of which the dielectric constants are $\varepsilon_{\rm P} = 3.23$, $\varepsilon_1 = 1$, $\varepsilon_2 = 2.8 + 0.001{\rm i}$, and ε_3, respectively. Here, the guiding layer has low dielectric loss, thus leading to a sharp decrease in the reflectivity when the leaky guiding mode is resonantly excited. For the Kerr medium, its dielectric constant depends on the square of the electric field E and can be expressed as $\varepsilon_3 = \varepsilon_{\rm L} + \alpha |E|^2$, where $\varepsilon_{\rm L}$ represents the linear dielectric constant of the substrate and $\alpha = c\varepsilon_0\varepsilon_{\rm L} n_{\rm NL}$ denotes the nonlinear coefficient, with $n_{\rm NL}$ being the optical Kerr nonlinear coefficient, c and ε_0 being the velocity of light and the permittivity of vacuum. The dielectric constant can also be rewritten as $\varepsilon_3 = \varepsilon_{\rm L} + \gamma |H|^2$, where $\gamma = c\mu_0 n_{\rm NL}$ (μ_0 denotes the permeability of vacuum) and H is the magnitude of the magnetic field component. In order to form a guiding mode, the refractive index of the waveguide should be larger than those of the gap layer and the substrate. In the following calculations, the parameters of the dielectric constant are set as $\varepsilon_{\rm L} = 2.46$ and $n_{\rm NL} = 2.0 \times 10^{-9}$ m^2/W.[18] The Kerr medium can be chosen as liquid crystal MBBA.[38]

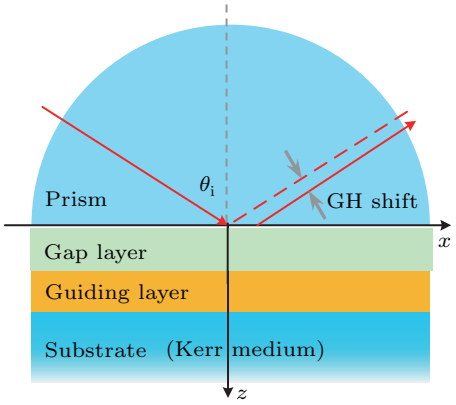


Fig. 1. Schematic of the GH effect in a slab waveguide structure composed of a prism, a gap layer, a waveguide layer, and a substrate with Kerr-type nonlinearity.

We consider a p-polarized light beam with wavelength $\lambda = 632.8$ nm incident from the prism onto the prism-gap interface (the coordinate plane of $z = 0$). When the guiding mode is resonantly excited in the waveguide, the evanescent field in the Kerr-type substrate is enhanced. Then, the intensity of the electromagnetic field at the waveguide-substrate interface is a crucial factor in analyzing the bistable reflection characteristics of the structure. Owing to the nonlinearity of the substrate, the dielectric constant varies with the penetration depth and the intensity of the electric (or magnetic) field. The wave equation for the magnetic field H_3 in the substrate can be derived from Maxwell's equations and is given by a second-order nonlinear differential equation[18]

$$\frac{{\rm d}^2 H_3}{{\rm d}z^2} + k_0^2(\gamma |H_3|^2 - q^2) H_3 = 0, \tag{1}$$

where $k_0 = 2\pi/\lambda$ is the wavenumber of the incident light in vacuum, and $q^2 = \varepsilon_{\rm P} \sin^2\theta_{\rm i} - \varepsilon_{\rm L}$, with $\theta_{\rm i}$ being the incident angle. The corresponding solution of Eq. (1) is

$$H_3 = \sqrt{\frac{2}{\gamma}} \frac{q \exp({\rm i}\phi_d)}{\cosh\left[qk(z - d_1 - d_2) + \kappa\right]}, \quad z \geq d_1 + d_2, \tag{2}$$

where $\phi_d = \arg(H_{3d})$, $\kappa = \cosh^{-1}(2q^2/\gamma |H_{3d}|^2)^{1/2}$, with H_{3d} being the amplitude of the magnetic field at the waveguide-substrate interface ($z = d_1 + d_2$). Then, the x component of the electric field can be expressed as

$$E_3 = \frac{{\rm i}qH_3}{\varepsilon_{\rm L} + \gamma |H_3|^2} \tanh\left[qk(z - \zeta) + \kappa\right]. \tag{3}$$

In order to obtain the relationship between the reflectivity and the input light intensity, as well as the internal electric-field profile of the structure, we use the transfer-matrix method. The relationship of electromagnetic fields between the plane of $z = 0$ and the plane of $z = d_1 + d_2$ is described as

$$\begin{pmatrix} H_1 \\ E_1 \end{pmatrix} = M \begin{pmatrix} H_{3d} \\ E_{3d} \end{pmatrix}, \tag{4}$$

where M is the characteristic transfer matrix composed of the gap layer and the guiding layer in the leaky waveguide structure. H_1 and E_1 are the tangential components of the magnetic field and the electric field at the prism-gap interface. Then, we can obtain the expressions of the reflection coefficient and the transmission coefficient as

$$r = \frac{(M_{11} + \eta_d M_{12})\eta_{\rm P} - (M_{21} + \eta_d M_{22})}{(M_{11} + \eta_d M_{12})\eta_{\rm P} + (M_{21} + \eta_d M_{22})}, \tag{5}$$

$$t = \frac{2\eta_{\rm P}}{(M_{11} + \eta_d M_{12})\eta_{\rm P} + (M_{21} + \eta_d M_{22})}, \tag{6}$$

where M_{ij} corresponds to the element of the transfer matrix M, $\eta_{\rm P} = \cos\theta_{\rm i}/\sqrt{\varepsilon_{\rm P}}$, and $\eta_d = E_{3d}/H_{3d}$. According to Eqs. (2) and (3), η_d is given by

$$\eta_d = \frac{{\rm i}q \tanh\kappa}{\varepsilon_{\rm L} + \gamma |H_d|^2}. \tag{7}$$

Once the amplitude of the magnetic field H_{3d} is known, we can obtain the input light intensity I_0 as

$$I_0 = \frac{1}{2\sqrt{\varepsilon_{\rm P}}\varepsilon_0 c} \left| \frac{H_d}{t} \right|^2. \tag{8}$$

Meanwhile, the reflectivity $R = |r|^2$ and the reflected phase shift $\Phi = \arg(r)$ can also be obtained. According to the stationary-phase theory,[2] the lateral displacement of the reflected light beam is given by

$$S_{\mathrm{GH}} = -\frac{1}{n_{\mathrm{P}} k_0} \frac{\mathrm{d}\Phi}{\mathrm{d}\theta_{\mathrm{i}}}. \tag{9}$$

Obviously, when the nonlinear coefficient α is 0, we have $\eta_d = (\varepsilon_{\mathrm{L}} - \varepsilon_{\mathrm{P}} \sin^2 \theta_{\mathrm{i}})^{1/2}/\varepsilon_{\mathrm{L}}$. Then, the reflection properties of the structure are independent of the intensity of the incident light. When the Kerr nonlinearity is taken into account, the reflectivity, phase shift, as well as the GH shift exhibit bistable behavior with respect to the input light intensity.

3. Results and discussion

Before embarking on a detailed analysis of the nonlinear response of the slab waveguide, we first consider the linear case in which the incident light is weak ($I_0 \approx 0$) and the nonlinear dielectric constant of the substrate is negligible. This corresponds to the initial state of the hysteresis loop. The reflectivity and reflected phase shift as functions of the incident angle are shown in Fig. 2. Generally, light incidents on the prism-gap interface with an angle larger than the critical angle is totally reflected. However, when the x-component of the wave vector in the prism matches the propagation constant of the guiding mode, the light energy can be coupled into the waveguide through the evanescent wave. Owing to the slight absorption of the waveguide, the reflection is attenuated, exhibiting the feature of FTR. Obviously, there is a sharp dip at the resonance angle $\theta_{\mathrm{R}} = 62.64°$. As the reflectivity reaches its minimum, the angular variation of the reflected phase shift reaches its maximum. According to Eq. (9), a large lateral displacement can be obtained in the resonance dip, while a small beam shift occurs out of resonance.

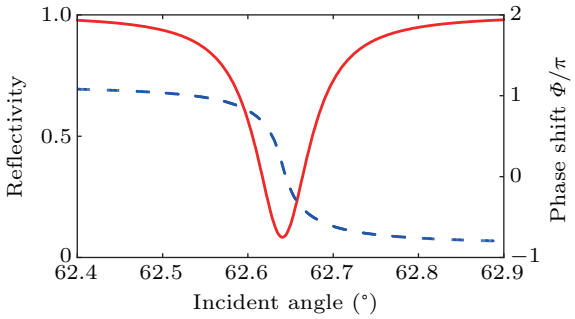


Fig. 2. Reflectivity (red solid line) and reflected phase shift (blue dashed line) as functions of the incident angle. The thicknesses of the gap layer and the guiding layer are $d_1 = 107$ nm and $d_2 = 401$ nm, respectively.

The nonlinear response of the reflection is illustrated in Fig. 3. Obviously, the reflectance and the GH shift exhibit hysteretic behavior. When a weak light beam is incident at an angle $\theta_{\mathrm{i}} = 62.79°$, which is slightly larger than the resonance angle $\theta_{\mathrm{R}} = 62.64°$, the waveguide mode cannot be excited, and the light is almost totally reflected (see the upper branch of the curve in Fig. 3(a)). As the intensity increases to a high threshold I_{h}, the waveguide is tuned toward resonance due to the change in the dielectric constant of the Kerr medium. As a result, the reflectance is switched from a high level (point B) to a low level (point C). Simultaneously, the GH shift jumps from a small value (point B) to a large one (point C), as shown in Fig. 3(b). When the input power is decreased, the output remains on the lower branch of the curve, and the reflectivity moves toward a minimum (point D). However, the nonlinear refractive index becomes so small at the low threshold I_{l} that the reflectance cannot maintain the FTR state, and this inherent feedback switches the system to the TIR state (point A). During this transition, the GH shift changes from large to small. Between the high and the low thresholds, both the reflectivity and the lateral displacement have two stable states and exhibit bistable behavior.

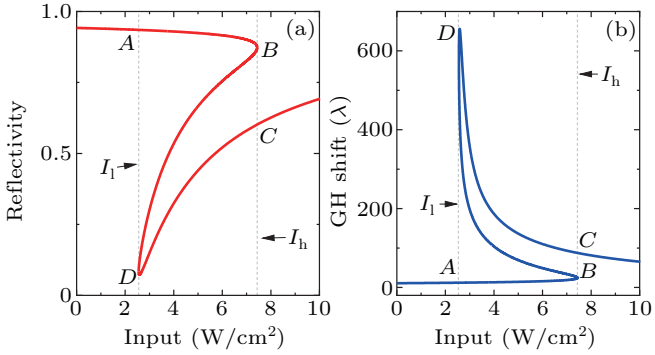


Fig. 3. (a) Reflectivity and (b) GH shift versus incident light intensity. The thicknesses of the gap layer and the guiding layer are $d_1 = 107$ nm and $d_2 = 401$ nm, respectively. The incident angle is $\theta_{\mathrm{i}} = 62.79°$.

According to the above discussions, the occurrence of optical bistability results directly from the intensity-dependent nonlinear refractivity of the substrate. During the switch-up and switch-down transitions between the two branches of the hysteresis loop, the electric field in the Kerr medium changes dramatically. We plot the electric-field intensity profile inside the four-layer waveguide structure in Fig. 4 to explain the hysteretic behavior. The reflectivity hysteresis curve in Fig. 3(a) can be divided into two processes: A–B–C with increasing input power, and C–D–A with decreasing input power. In the process A–B, the intensity of the surface electric field in the substrate increases slowly with the input power, shifting the resonance angle θ_{R} toward the incident angle θ_{i}. When the system gradually enters the waveguide mode (point B), the internal electric field increases abruptly as a result of the positive feedback effect, which causes the reflectance curve to switch from TIR below θ_{R} to FTR slightly above θ_{R}. Accordingly, the reflectivity jumps from point B to point C. In the process C–D, the system still remains in the FTR state and approaches resonance with decreasing incident intensity. At point D, the input power reaches the minimum required intensity for the resonant mode. When the input power decreases further, the

internal electric field decreases abruptly, leading to the system moving suddenly away from resonance. Then, the system returns from the FTR state to the TIR state. During these processes, the lateral displacement associated with the phase variation also exhibits bistable behavior. The enhancement of the GH effect is related to the increase of the evanescent field in the structure. In the process *A*–*B*, the internal evanescent electric field is weak due to the off-resonance condition. In the process *C*–*D*, the evanescent electric field is enhanced by the excitation of the waveguide mode, so the lateral displacement is correspondingly enlarged. Especially near point *D*, the waveguide mode is fully excited, resulting in a significant change in the phase shift. Then, the GH shift can reach a maximum value and exhibits a peak near the low threshold $I_{\rm l}$, as shown in Fig. 3(b).

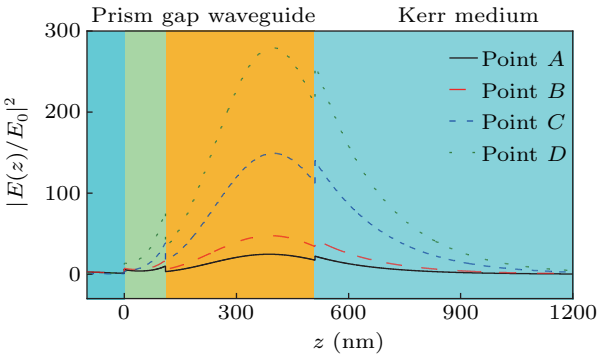


Fig. 4. Electric-field distributions $E(z)$ in the slab waveguide structure at the points marked *A*–*D* in Fig. 3. E_0 is the amplitude of the incident electric field.

In the prism-coupled waveguide structure, the complex propagation constant of the leaky waveguide mode consists of two parts: β, the eigen propagation constant of the three-layer waveguide (assuming the gap layer is infinite), and $\Delta\beta$, the offset of the propagation constant caused by the gap layer with finite thickness.[21] Their imaginary parts represent the intrinsic loss resulting from the absorption of the waveguide ($\Gamma_{\rm i} = {\rm Im}(\beta)$) and the radiation loss caused by the gap layer ($\Gamma_{\rm r} = {\rm Im}(\Delta\beta)$). Therefore, under the condition $|\exp(2{\rm i}k_{1z}d_1)| \ll 1$ (k_{1z} is the z component of the wave vector in the gap layer), the reflectivity and GH shift of the leaky waveguide structure have the form[21]

$$R = 1 - \frac{4\Gamma_{\rm i}\Gamma_{\rm r}}{\Delta^2 + (\Gamma_{\rm i}+\Gamma_{\rm r})^2}, \tag{10}$$

$$S_{\rm GH} = -\cos\theta \frac{2\Gamma_{\rm r}(\Gamma_{\rm i}^2 - \Gamma_{\rm r}^2 - \Delta^2)}{4\Delta^2\Gamma_{\rm r}^2 + (\Gamma_{\rm i}^2 - \Gamma_{\rm r}^2 + \Delta^2)^2}, \tag{11}$$

where $\Delta = k_x - {\rm Re}(\beta + \Delta\beta)$, and $k_x = \sqrt{\varepsilon_{\rm P}}k_0 \sin\theta_{\rm i}$ is the x component of the incident wave vector. When $\Delta = 0$, the system satisfies the phase-matching condition, $\theta_{\rm i} = \theta_{\rm R}$, and the reflectivity and GH shift can be written as

$$R_{\rm min} = \left(\frac{\Gamma_{\rm i} - \Gamma_{\rm r}}{\Gamma_{\rm i} + \Gamma_{\rm r}}\right)^2, \tag{12}$$

$$S_{\rm GH} = \frac{2\Gamma_{\rm r}}{\Gamma_{\rm r}^2 - \Gamma_{\rm i}^2}\cos\theta_{\rm R}. \tag{13}$$

Therefore, ${\rm Re}(\beta + \Delta\beta)$, the eigen propagation constant of the system, determines the resonance angle $\theta_{\rm R}$, while the intrinsic loss $\Gamma_{\rm i}$ and the radiation loss $\Gamma_{\rm r}$ together determine the minimum reflectivity $R_{\rm min}$. The losses $\Gamma_{\rm i}$ and $\Gamma_{\rm r}$ also affect the lateral displacement. According to Eq. (13), a small difference between $\Gamma_{\rm i}$ and $\Gamma_{\rm r}$ corresponds to a small $R_{\rm min}$ and a large $S_{\rm GH}$. The complex propagation constant depends on the thickness and permittivity of the layers. Therefore, $\theta_{\rm R}$ and $S_{\rm GH}$ vary with these system parameters, which accordingly affect the hysteretic response. In the following, we investigate the influence of the layer thickness on the bistability of the GH shift.

Firstly, we investigate the effect of the thickness of the gap layer d_1 on the bistability when the thickness of the guiding layer is fixed. The reflectance and phase-shift spectra with different d_1 are shown in Fig. 5 under the condition of weak input, which corresponds to the initial state of the hysteresis loop ($I_0 \approx 0$). As d_1 increases, the resonance angle $\theta_{\rm R}$ decreases gradually owing to the decreasing offset propagation constant $\Delta\beta$. Meanwhile, the energy leakage from the waveguide to the prism is reduced, thereby decreasing the radiation loss $\Gamma_{\rm r}$. As a result, the minimum reflectivity $R_{\rm min}$ becomes smaller, and the rate of change of the phase ${\rm d}\Phi/{\rm d}\theta_{\rm i}$ at resonance tends to increase, as shown in Fig. 5(b).

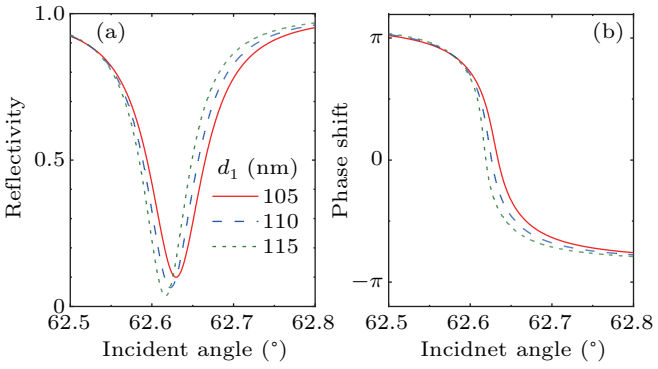


Fig. 5. (a) Reflectivity and (b) reflected phase shift versus incident angle for different thicknesses of the gap layer d_1. The thickness of the guiding layer is $d_2 = 401$ nm.

Considering the Kerr nonlinearity of the substrate, we plot the nonlinear GH shift as a function of the incident light intensity, as shown in Fig. 6. In the case that the incident angle $\theta_{\rm i}$ is larger than the resonance angle $\theta_{\rm R}$, the initial angle offset, $\Delta\theta = \theta_{\rm i} - \theta_{\rm R}$, increases with the thickness d_1. Then, a larger input power is necessary to bring $\theta_{\rm R}$ into coincidence with $\theta_{\rm i}$, leading to an increase in the switching threshold $I_{\rm h}$. The peak value of the GH shift near the low threshold $I_{\rm l}$ is related to the exact excitation of the waveguide mode. For large d_1, the minimum reflectivity becomes smaller and the phase variation becomes sharper (see Fig. 5). As a result, a larger lateral displacement can be obtained with a thicker gap layer.

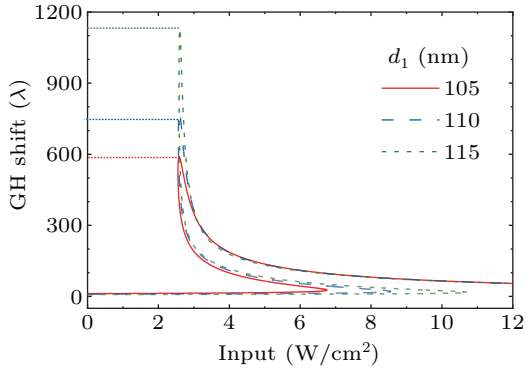


Fig. 6. GH shift versus incident intensity for different thicknesses of the gap layer at a fixed incident angle $\theta_i = 62.79°$. The thickness of the guiding layer is $d_2 = 401$ nm.

Secondly, we investigate the influence of the thickness of the guiding layer d_2 on the bistability. Under the condition of weak input, the reflectivity and phase-shift spectra versus the incident angle for different d_2 are plotted in Fig. 7. With the increase of d_2, the real part of the propagation constant of the waveguide, i.e., $\mathrm{Re}(\beta + \Delta\beta)$, increases accordingly, thus resulting in a rightward shift of the resonance angle. However, the changes in the minimum reflectivity as well as the variation of the phase in the FTR dip are small. Therefore, we can expect that when the incident light excites the waveguide mode, the corresponding GH shift peak does not change significantly.

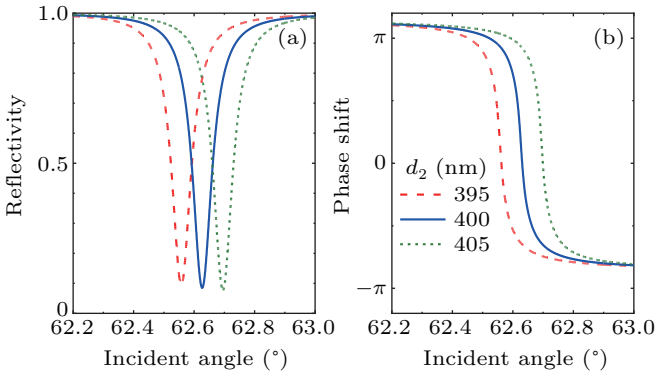


Fig. 7. (a) Reflectivity and (b) phase shift versus incident angle for different thicknesses of the guiding layer d_2. The thickness of the gap layer is $d_1 = 107$ nm.

The nonlinear GH shifts versus the incident light intensity for different thicknesses of the guiding layer are shown in Fig. 8. It has been previously analyzed that the increase in the thickness of the guiding layer leads to a rightward shift of the resonance angle, and then the initial angle offset $\Delta\theta$ is small for large d_2. Therefore, a smaller input power can switch the hysteresis of the GH shift from the lower to the upper branch. That is, I_h, the threshold intensity for the transition from the TIR state to the FTR state, is reduced with the increase of d_2. The peak values of the GH shift, as predicted above, are almost unchanged. In Fig. 9, we plot the internal electric field profiles at the three peak points. As d_2 increases, the losses of the waveguide decrease, resulting in a decrease of the minimum electric field intensity required to maintain the waveguide mode. Therefore, the minimum input required to remain in the FTR state is decreased, thus reducing the low threshold I_l. Furthermore, if d_2 is further increased, the optical bistability will disappear. In this case, the initial angle offset is so small that the nonlinear GH shift has only a single-valued relationship with the input intensity.

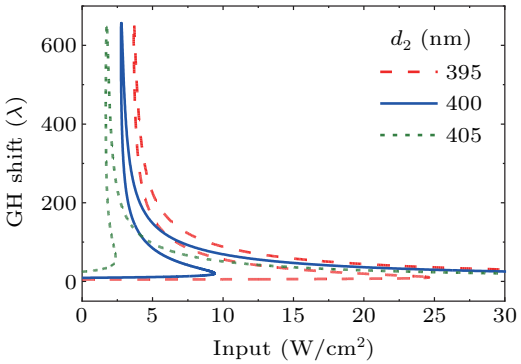


Fig. 8. GH shift versus incident intensity for different thicknesses of the guiding layer at a fixed incident angle $\theta_i = 62.79°$. The thickness of the gap layer is $d_1 = 107$ nm.

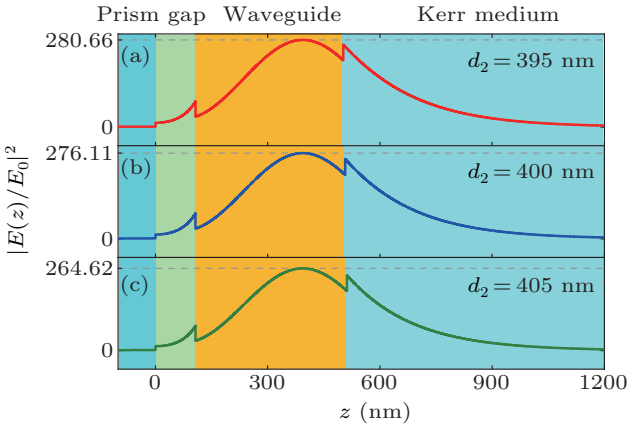


Fig. 9. Electric field distribution $E(z)$ at the three peak points of the GH shift shown in Fig. 8. E_0 is the amplitude of the incident electric field.

So far, we have studied the nonlinear lateral shift with different thicknesses of the gap layer and guiding layer. Further calculations were carried out to evaluate the range of thicknesses of the gap layer and waveguide within which a bistable hysteresis loop can be obtained. The ranges of d_1 and d_2 exceed 30 nm and 20 nm, respectively, while for a large thickness of the gap layer ($d_1 > 122$ nm) and a small thickness of the waveguide ($d_2 < 390$ nm), the thresholds increase significantly. Therefore, the bistable GH shift can be observed conveniently under a wide range of parameters, which are much larger than the tolerance of the preparation precision of thin films and the control of the gap layer (the accuracy of film thickness can reach $\pm 0.5\%$).

In Fig. 10, we show the influence of the incident angle on the bistable response of the GH shift. The reflectivity and phase shift spectra with a weak input are shown in Fig. 2 and the initial resonance angle is $\theta_R = 62.64°$. As the incident angle θ_i increases, the initial angle offset $\Delta\theta$ also increases. Therefore, a larger input power is necessary

to shift the intensity-dependent θ_R toward θ_i, thus increasing both thresholds I_h and I_l. However, I_h increases faster than I_l. At the three peak points, the eigen loss and radiation loss of the structure are almost the same, and therefore there are only slight changes in the peak values of the GH shift. The minimum incident angle at which optical bistability can occur is about $\theta_i = 62.72°$. The optimal incident angle should be less than 62.9°, exceeding which the thresholds become too large. In a real experiment, the offset angle $\Delta\theta$ can be flexibly tuned below 0.1°.[38] Therefore, the tolerance angle of the leaky waveguide is large enough.

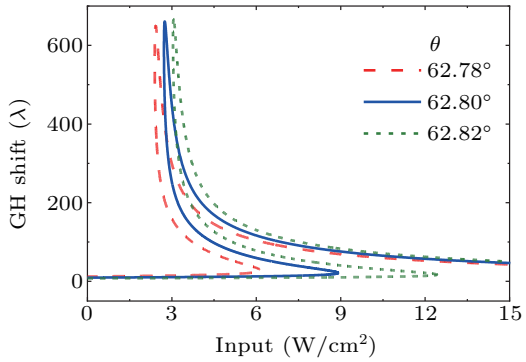


Fig. 10. Bistable GH shift for different angles of incidence. The thicknesses of the gap layer and the guiding layer are $d_1 = 107$ nm and $d_2 = 401$ nm, respectively.

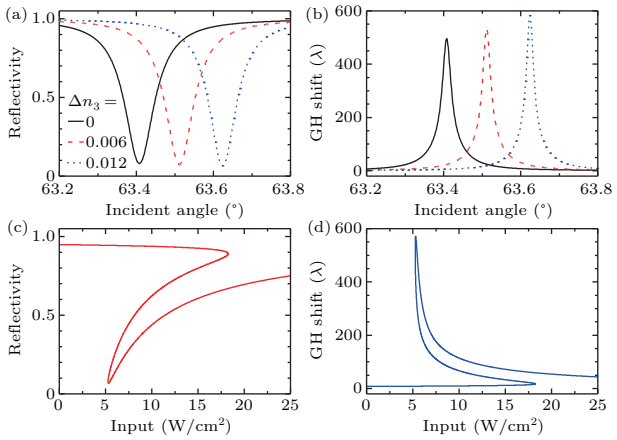


Fig. 11. (a) and (b) Angular spectra of reflectivity and GH shift for different refractive indices of the substrate when the incident light is s-polarized. (c) and (d) Bistable reflectivity and GH shift with a Kerr substrate. The thicknesses of the gap layer and the guiding layer are $d_1 = 160$ nm and $d_2 = 401$ nm, respectively. The incident angle is $\theta_i = 63.60°$.

Compared with metal-based devices using surface plasmon polaritons, which support optical resonance only for p-polarized incident light, the leaky mode can be excited by both p- and s-polarized light impinging upon the waveguide system. In Figs. 11(a) and 11(b), we plot the reflectivity and lateral shift of an s-polarized light beam. The typical ATR feature is clearly observed due to the excitation of the guiding mode. When the refractive index of the substrate increases, the resonance angle shifts to the right. For an incident angle $\theta_i = 63.60°$, the reflectivity can be switched between two stable states, ATR and TIR, by varying the incident light intensity to modulate the Kerr nonlinear refractivity, as shown in Fig. 11(c). Simultaneously, the GH shift also exhibits a hysteretic response (see Fig. 11(d)).

A potential application of the bistable GH shift is in optical switching, where the transient process and response speed are crucial. Because the structures of the waveguide and the SPR system are similar, the response times associated with the excitation of the leaky mode and surface plasmon polariton are on the same order, mainly determined by the nonlinear material and the structure.[41] For a liquid crystal Kerr medium, the response time ranges from 10 μs to 1 s. For a solid nonlinear crystal, the response time is usually less than 1 ns, even down to the order of ps. Therefore, the typical response time of the structure can reach sub-ps levels.[42]

4. Conclusion

In summary, we have investigated the nonlinear GH shift in a prism-coupled slab waveguide with a Kerr nonlinear substrate. Owing to the positive feedback effect induced by the intensity-dependent guiding mode, there exist two switchable stable states, total internal reflection and frustrated total reflection. The lateral displacement exhibits a hysteretic response to the input power. As the incident intensity varies, the waveguide is tuned in and out of resonance, corresponding to states with large and small GH shift, respectively. When the input power slightly exceeds the low threshold, the lateral shift can be greatly enhanced and the reflectivity reaches a minimum due to the matching between the tangential component of the wave vector in the prism and the intensity-dependent propagation constant of the waveguide mode. It is also found that the hysteresis loop depends strongly on system parameters, such as the thicknesses of the gap and guiding layers, and the incident angle. The gap layer affects the radiation loss of the leaky waveguide and the resonance angle, thereby influencing the peak value of the bistable GH shift and shifting the high threshold. The guiding layer mainly affects the initial resonance angle, thereby modifying both the low and high thresholds. The bistable behavior of the GH shift may find applications in all-optical devices.

Acknowledgment

This work was supported by the Natural Science Foundation of Jilin Province of China (Grant No. 20220101031JC).

References

[1] Goos F and Hänchen H 1947 *Ann. Phys.* **436** 333
[2] Artmann K 1948 *Ann. Phys.* **437** 87
[3] Yu T, Li H, Cao Z, Wang Y, Shen Q and He Y 2008 *Opt. Lett.* **33** 1001
[4] Wu Y, Wu L and Ang L K 2024 *Opt. Express* **32** 11171

[5] Luo M and Wu F 2024 *Phys. Rev. Applied* **22** 014050
[6] Sakata T, Togo H and Shimokawa F 2000 *Appl. Phys. Lett.* **76** 2841
[7] Chen X M, Shui T, Meng C, Zhang T, Deng X and Yang W X 2021 *Laser Phys. Lett.* **18** 045205
[8] Kar A, Goswami N and Saha A 2017 *Appl. Opt.* **56** 9656
[9] Wang L G and Zhu S Y 2005 *Appl. Phys. Lett.* **87** 221102
[10] Li C F 2003 *Phys. Rev. Lett.* **91** 133903
[11] Lai H M and Chan S W 2002 *Opt. Lett.* **27** 680
[12] Yan Y, Chen X and Li C F 2007 *Phys. Lett. A* **361** 178
[13] Provenzano D B and la Rocca G C 2024 *Phys. Rev. A* **110** 033514
[14] Jiang L Y, Wang Q K, Xiang Y J, Dai X Y and Wen S C 2013 *IEEE Photon. J.* **5** 6500108
[15] You Q, Jiang L Y, Dai X Y and Xiang Y J 2018 *Chin. Phys. B* **27** 094211
[16] Zeng X D, Al-Amri M and Zubairy M S 2017 *Opt. Express* **25** 23579
[17] Yin X B, Hesselink L, Liu Z W, Fang N and Zhang X 2004 *Appl. Phys. Lett.* **85** 372
[18] Zhou H C, Chen X, Hou P and Li C F 2008 *Opt. Lett.* **33** 1249
[19] Salasnich L 2012 *Phys. Rev. A* **86** 055801
[20] Wan R G and Zubairy M S 2020 *Opt. Express* **28** 6036
[21] Liu X B, Cao Z Q, Zhu P F, Shen Q S and Liu X M 2006 *Phys. Rev. E* **73** 056617
[22] Chen L, Zhu Y M, Zhang D W, Cao Z Q and Zhuang S L 2009 *Chin. Phys. B* **18** 4875
[23] You Q, Guo J, Wu L M, Dai X Y and Xiang Y J 2018 *Chin. Phys. B* **27** 087302
[24] Wan R G and Zubairy M S 2020 *Phys. Rev. A* **101** 023837
[25] He Y Q, Luo X X, Shui T and Yang W X 2025 *Appl. Phys. B* **131** 88
[26] Wang L G, Ikram M and Zubairy M S 2008 *Phys. Rev. A* **77** 023811
[27] Abbs M, Asadpour S H, Ziauddin, Zhang P, Ruseckas J and Hamedi H R 2024 *Phys. Rev. A* **110** 023730
[28] Liu X, Wang Y X and Wu J H 2025 *Opt. Express* **33** 9937
[29] Jiang X W, Fang B and Zhan C L 2024 *Chin. Phys. B* **33** 034206
[30] Liu J Q, Zheng Y, Li X, Li J W, Zhang G H, Dong D X, Liu D M, Jia Y W, Fu Y Y and Liu Y W 2025 *Chin. Phys. B* **34** 074208
[31] Gibbs H M, McCall S L and Venkatesan T N C 1976 *Phys. Rev. Lett.* **36** 1135
[32] Harshawardhan W and Agarwal G S 1996 *Phys. Rev. A* **53** 1812
[33] Wysin G, Simon J and Deck R 1981 *Opt. Lett.* **6** 30
[34] Hickernell R and Sarid D 1986 *J. Opt. Soc. Am. B* **3** 1059
[35] Cai Y P and Wan R G 2022 *Opt. Express* **30** 20725
[36] Avinash K, Goswami N and Saha A 2023 *Appl. Opt.* **62** 3797
[37] Montemayor V and Deck R 1985 *J. Opt. Soc. Am. B* **2** 1010
[38] Dannberg P and Broese E 1988 *Appl. Opt.* **27** 1612
[39] Xu G D, Zang T C, Mao H M and Pan T 2010 *Phys. Lett. A* **374** 3590
[40] Kar A, Goswami N and Saha A 2019 *Appl. Opt.* **58** 9376
[41] Herminghaus S and Schmidt H J 1994 *Opt. Lett.* **19** 293
[42] Min C, Wang P, Chen C, Deng Y, Lu Y, Ming H, Ning T, Zhou Y and Yang G 2008 *Opt. Lett.* **33** 869